Transient IR ($00^0$1-$00^0$0) Absorption Spectroscopy of Optically Centrifuged N_2O with Extreme Rotation up to J=205

Hannah M. Ogden, Tara J. Michael, Matthew J. Murray and Amy S. Mullin*

Department of Chemistry and Biochemistry, University of Maryland, College Park, MD, USA 20742

*Corresponding author

Email addresses: hogden@umd.edu, tarajade@umd.edu, matthew.murray@nrl.navy.mil, mullin@umd.edu

Abstract

High-resolution transient IR absorption spectroscopy was used to measure ($00^0$1−$00^0$0) R-branch transition frequencies for N_2O molecules in extreme rotational states, with quantum number up to J = 205 and energies as high as E_{rot}=17000 cm^{-1}. A population inversion of rotationally excited N_2O states was prepared with an optical centrifuge and probed in a multi-pass IR cell using a quantum cascade laser. The optical centrifuge is based on 800-nm ultrafast, chirped laser pulses that optically trap molecules and accelerate them angularly to extreme rotational states. This work substantially increases the range of observed transitions for this band beyond J = 100 transitions previously reported and provides benchmark measurements for theoretical predictions based on a polyad model of effective Hamiltonian. Transient Doppler-broadened IR line profiles of N_2O show that optical excitation of the sample is selectively partitioned into rotation, prior to Doppler broadening from rotation-to-translation collisional energy transfer. These results demonstrate how high-J transitions can be measured without thermal heating by coupling optical centrifuge excitation with high-resolution transient IR absorption probing.

Keywords: Nitrous oxide, high temperature, optical centrifuge, transient IR probing, extreme rotation, super rotors

1. Introduction

High-resolution spectroscopy is a powerful tool for characterizing the temperature of plasmas, flames, combustion engines and exoplanet atmospheres. Heating a gas makes it possible to observe transitions from highly excited states that are not populated at ambient temperatures. However, heating can also lead to spectral congestion and line broadening that complicate and obscure otherwise well-resolved spectra. An alternative approach to heating is to use an optical centrifuge to selectively populate high energy rotational states, without directly exciting the vibrational and translational degrees of freedom in a molecule. An optical centrifuge is based on intense ultrafast laser pulses that trap molecules and accelerate them angularly into high rotational states. Here, we have prepared high-J states of the main isotope of N_2O with an optical centrifuge and measured (00^01-00^00) R-branch transitions for a number of states with J = 95-205 using high-resolution transient IR absorption spectroscopy.

Nitrous oxide, N_2O, is an important species in many environments and high-resolution IR spectra have been reported previously for transitions with $J \leq 100$. In 1987, Toth reported IR transitions involving states up to J = 92 at 300 K [1]. A number of studies have reported molecular constants for vibrational hot bands [2–5]. In 2011, we extended the experimental observation of N_2O (00^00) ν_3 transitions to R100 using optical centrifuge excitation and single-pass transient IR detection [6]. In 2014, Ting et al. also reported ν_3 transition frequencies up to R100 with 10 kHz precision [7]. Here, we extend the observed transitions to R205, made possible by the addition of a multi-pass IR detection cell to the optical centrifuge spectrometer.

In lieu of experimental observations of high-J transitions for N_2O, the high-temperature spectrum has been calculated with global modeling of line positions using a polyad model of effective Hamiltonian [8]. This approach yields 138 effective Hamiltonian parameters and successfully reproduces accurate line positions for more than 37,000 measured line positions of 325 vibrational bands. Two high-temperature spectral databases, NOSD-1000 and HITEMP, include calculated IR transitions for high-J transitions of N_2O [9,10]. The maximum J-state listed in the HITEMP database is near J =100.

Line positions for ν_3 transitions were calculated up to $J = 205$ from the set of effective Hamiltonian parameters developed by V.I. Perevalov and coworkers [8]. Line positions from the effective Hamiltonian calculations are identified here as ν_{calc}. We also extrapolated high-J transitions, identified here as ν_{ext}, from low-J HITRAN data [11]. Molecular constants were determined from data for $J \leq 90$ using an energy expansion in $J(J+1)$ where $E_n(J) = v_n + B_n J(J+1) - D_n(J(J+1))^2 + H_n(J(J+1))^3$ and n is the number of quanta in the ν_3 mode. The molecular constants in units of cm^{-1} are $v_0 = 0$, $B_0 = 0.41901$, $D_0 = 1.7609 \times 10^{-7}$, $H_0 = -1.6687 \times 10^{-14}$, $v_1 = 2223.757$, $B_1 = 0.41556$, $D_1 = 1.7547 \times 10^{-7}$ cm^{-1}, and $H_1 = -1.3351 \times 10^{-14}$. The observed transitions ν_{obs} are compared to both calculated line positions ν_{calc} and extrapolated line positions ν_{ext}.

A portion of the calculated R-branch transitions is shown in Fig. 1 based on a 1000 K distribution. A band head is seen at R116 and transitions for higher J-states lie between known lower-J transitions. We use this feature to measure new high-J transitions with spectral fingerprinting.

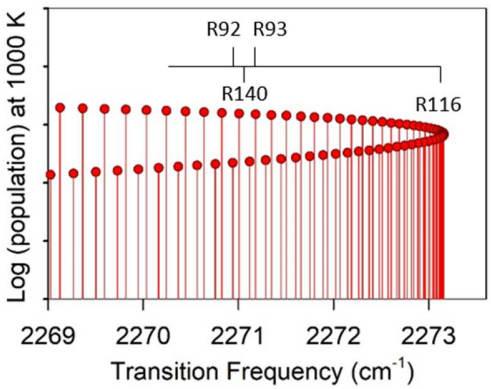

Fig. 1. Calculated ν_3 R-branch transitions for high-J states of N_2O. Transitions have been observed previously up to J = 100.

2. Experimental Methods

Fig. 2 shows a schematic diagram of the optical centrifuge transient IR absorption spectrometer. In the work reported here, an optical centrifuge was used to excite a 300 K sample of N_2O into extreme rotational states with oriented angular momentum. High-resolution transient IR absorption spectroscopy of individual rotational states was performed with a quantum cascade laser, a multi-pass detection cell and active feedback control of the IR wavelength. The optical centrifuge spectrometer has been described in detail previously [12] and the key features are given below.

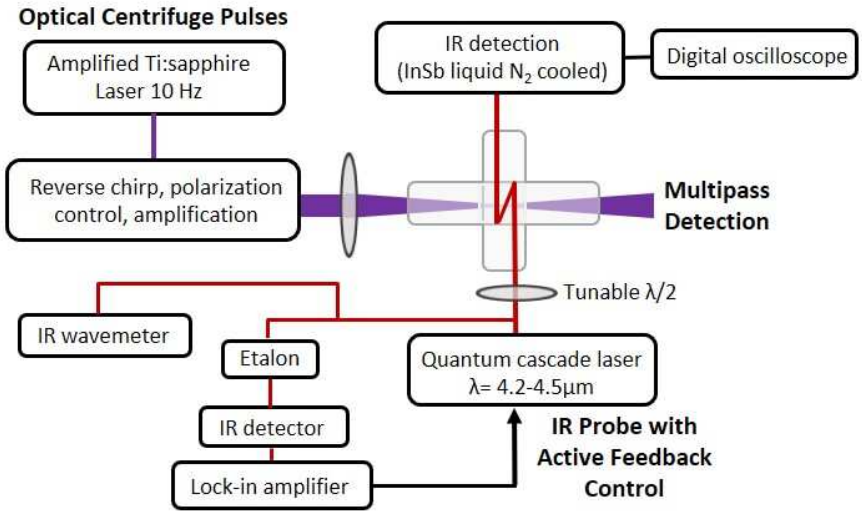

Fig. 2. Overview of the optical centrifuge transient IR absorption spectrometer. The optical centrifuge pulses excite N_2O molecules into extreme rotational states with classical rotational frequencies up to $\Omega_{OC} = 5 \times 10^{13}$ rad s^{-1}. Transient IR probing detects population changes in N_2O (00^00) rotational states from the centrifuge pulse.

2.1 Optical centrifuge excitation of N_2O (00^00)

The optical centrifuge is created by combining two oppositely-chirped ultrafast laser pulses, each with opposite circular polarization [13,14]. The resulting linearly polarized light accelerates angularly over the time of the pulse. Molecules with non-uniform polarizability are trapped in the optical field by an induced-dipole interaction such that the angle θ between the molecular and optical axes goes to zero, as illustrated in Fig. 3a. The aligned molecules are spun into high rotational states with unidirectional motion by the angular acceleration of the optical field.

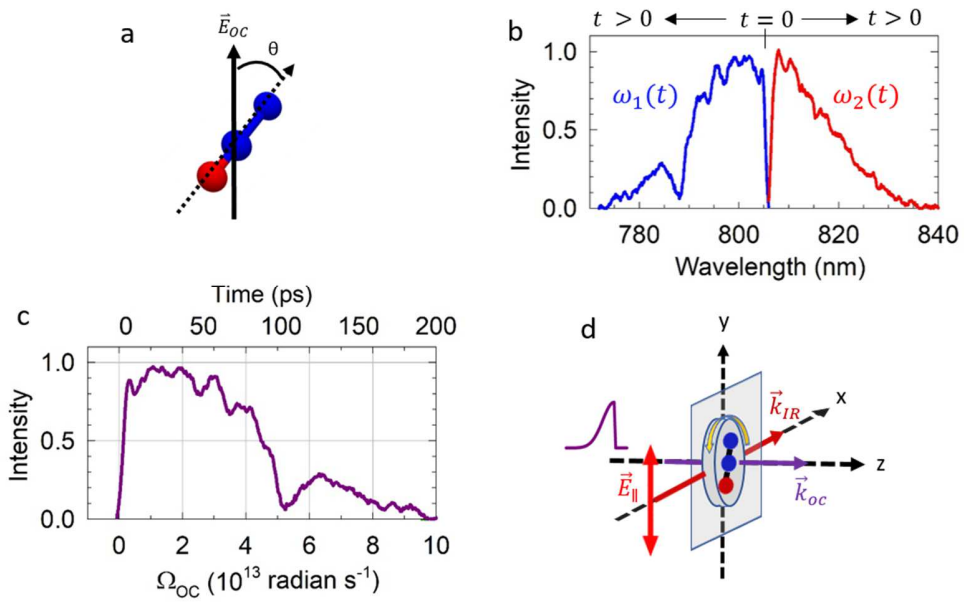

Fig. 3. a) N_2O molecules are aligned in the optical centrifuge field before being driven into high rotational states. b) Spectrum of the chirped pulses that form the optical centrifuge. c) Intensity of the optical centrifuge field as a function of angular frequency. d) Geometry of the optical centrifuge IR-probing interaction region. The centrifuge beam propagates along the z-axis (indicated by $\vec{k}_{oc}$) and the IR probe beam propagates along the x-axis (indicated by $\vec{k}_{IR}$). The IR probe polarization is parallel to the plane of molecular rotation (indicated by $\vec{E}_{\parallel}$).

The centrifuge pulses originate from an amplified Ti:sapphire ultrafast laser system (Coherent) that generates pulses of light centered near λ_0 = 805 nm at a repetition rate of 10 Hz. The pulses are stretched to a pulse width of 100 ps, spectrally cut in half, given opposite chirp, and further amplified. The two oppositely chirped pulses, with counter-rotating circular polarization, are overlapped spatially and temporally to produce the angularly accelerating field.

The combined pulses are focused to a beam waist of 52 μm with an intensity of 3×10^{13} W cm^{-2}.

The spectrum of the oppositely chirped pulses is shown in Fig. 3b, where the positively and negatively chirped pulses are shown as $\omega_1(t)$ and $\omega_2(t)$, respectively. The trap intensity is shown in Fig. 3c as a function of instantaneous angular frequency Ω_{OC} where $\Omega_{OC}(t) = \big(\omega_1(t) - \omega_2(t)\big)/2$. Molecules trapped in the optical centrifuge rotate at the same frequency as the field such that $\Omega_{OC} = \Omega_J$. Molecules are released from the optical trap when the trap intensity is insufficient to drive them into higher angular momentum states. For these measurements, an optical coating flaw at λ =788 nm led to a drop in trap intensity near $\Omega_{OC} = 5 \times 10^{13}$ rad s^{-1}. An N_2O molecule spinning in the optical field at $\Omega_{OC} = 4.2 \times 10^{13}$ rad s^{-1} corresponds to a rotational state of $J \approx 205$ with $E_{rot} > 17000$ cm^{-1}.

2.2 High-resolution transient IR absorption spectrometer

The optical centrifuge is coupled to a high-resolution transient IR absorption spectrometer to measure the appearance of molecules in high-J states and identify new spectral lines. The geometry of the interaction region is shown in Fig. 3d. The optical centrifuge pulses propagate along the z-axis (indicated by $\vec{k}_{oc}$) and prepare rotationally excited N_2O molecules that rotate in the xy-plane. The IR probe beam propagates along the x-axis (indicated by $\vec{k}_{IR}$), crosses the centrifuge beam 11 times and has polarization that is parallel $(\vec{E}_{\parallel})$ to the xy-plane. For an unfocused input optical centrifuge beam diameter of 0.48 cm, the IR path length in the interaction region is $\ell = 0.12$ cm.

The IR probe is a single-mode quantum cascade laser (Daylight Solutions) operating between λ = 4.2 – 4.5 μm with a frequency resolution of $\Delta\nu_{IR} < 2 \times 10^{-4}$ cm^{-1}. Transient

absorption signals for individual J-states were collected on a liquid nitrogen cooled InSb detector and averaged on a digital oscilloscope. A number of R-branch transitions were measured for states with J = 92-205. The output of the IR laser ends just beyond the R205 transition. The cell pressure is 5 Torr, for which the average time between collisions is approximately 20 ns. Collision numbers reported in this paper are based on a hard-sphere collision rate constant of $k_{col} =$ 2.5×10^{-10} cm^3 molecule^{-1} s^{-1} and a collision cross section of $\sigma = 0.47$ nm^2 [15]. The Lennard-Jones collision rate constant is a factor of two larger, so collision numbers reported here should be considered as lower limits. Transient signals measured at t = 60 ns after the centrifuge pulse correspond to populations that have undergone 3 collisions on average. Spectroscopic grade N_2O (99.99% purity) was used.

IR transition frequencies were determined using high-resolution transient spectral fingerprinting and a wave meter with an effective resolution that is better than $\Delta\nu_{wm}$= 1 × 10^{-3} cm^{-1}. The wave meter is internally calibrated using a stabilized HeNe transition. Transient fingerprint spectra were recorded by starting at a known N_2O transition and stepping the IR frequency in steps of $\delta_\nu < 0.001\ cm^{-1}$. Control of the IR wavelength was achieved by locking the output of the IR laser to a fringe of a tunable Fabry-Perot etalon using active feedback control. The accuracy of the wave meter readings was established by locking the IR probe laser to a transition involving a thermally populated N_2O state and comparing with known transition frequencies.

Transient Doppler-broadened line profiles were measured for a number of N_2O states. Transient signals were collected at discrete IR wavelengths as the probe laser was tuned across the line profile in approximately 40 steps. Doppler profiles at discrete times were fit to Gaussian

functions and time-dependent translational temperatures were extracted from the widths of the fitted profiles.

3. Results

Here we report transition frequencies for N_2O (00^01-00^00) R-branch transitions with $J =$ 140-205 using transient IR absorption spectroscopy. Line positions were determined using spectral fingerprinting for four transitions. Line positions for 7 additional transitions were measured with the wave meter. Transient Doppler profiles were measured as a function of J to show how line widths are affected by optical centrifuge excitation.

3.1 Transient (00^01-00^00) spectroscopy of optically centrifuged N_2O

Fig. 4a shows the transient absorption signal at line center for the R140 transition near 2271 cm^{-1}. Fig. 4b shows the transient spectral fingerprinting for R92, R140 and R93 at three times following the centrifuge pulse. The fingerprint scans show that the R140 intensity increases from $t = 60$ to 120 ns and then decreases at $t = 200$ ns, while the R92 and R93 intensities increase ten-fold from t = 60 ns to 200 ns. The population changes arise from rotational energy transfer as the optically centrifuged molecules return to equilibrium populations through collisions. The initial increase in the R140 signal shows that the centrifuge pulse initially prepares molecules in states higher than J=140 and population passes through this state during the relaxation process.

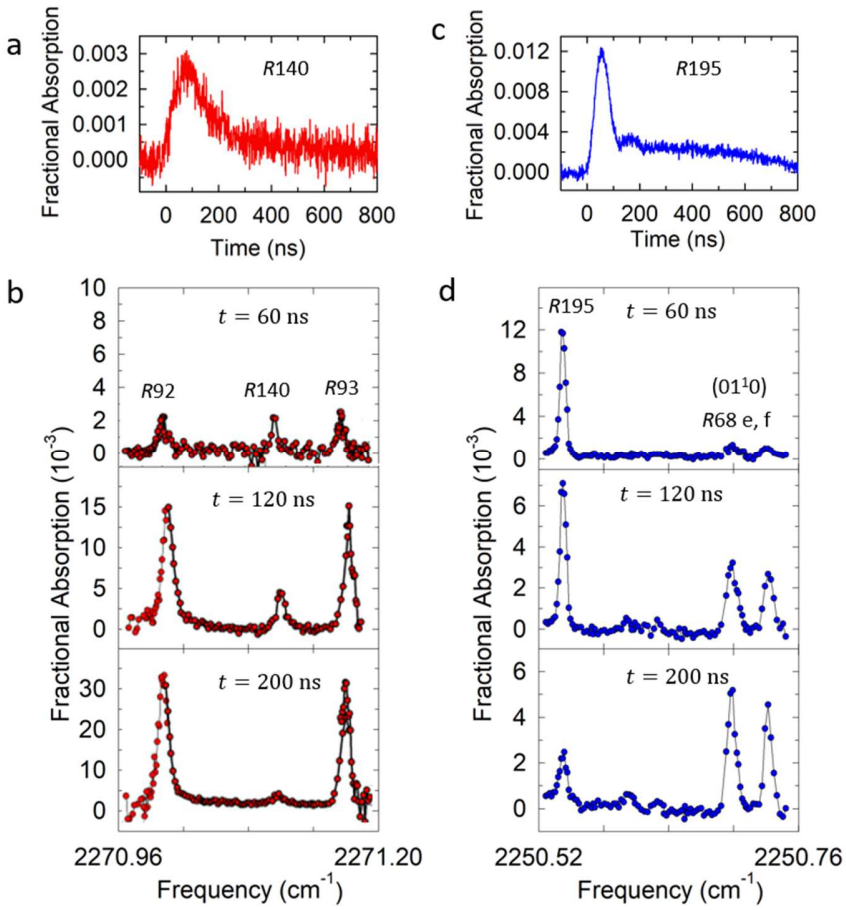

Fig. 4. Line-center transient absorption measurements for a) R140 and c) R195 of N_2O. Transient fingerprint scans at t = 60, 120, and 200 ns after optical centrifuge excitation for b) R140 and d) R195.

Fig. 4c shows the line center transient signal for R195. Two components are present: a prompt population that is formed in the centrifuge and a slow population that comes from collisional cooling of centrifuged molecules. Spectral fingerprinting for R195 uses R68 *e,f* transitions of the (01^11-01^10) band, as shown in Fig. 4d. The R195 transition is most intense at $t = 60$ ns and decreases by a factor of four at $t = 200$ ns. Population in the bending state increases by a factor of 3 over the same time period as a result of collisional energy transfer. The time-dependent scans show how population is initially created in high-J states with the optical

centrifuge pulse and then collisions redistribute the energy into lower rotational states and possibly vibrational states that are not easily populated with traditional optical methods. The N_2O (01^10) bending mode can be populated by rotation-to-vibration/rotation energy transfer from the (00^00) state or by rotational excitation of (01^10) state that is 8% of vibrational distribution at 300 K. In other optical centrifuge experiments, we have detected transient absorption of CO_2 (03^30) P43, resulting from collisions, so it is likely that the one quantum of the bend for N_2O is also populated by collisions [16].

Absolute line center frequencies ν_{obs} were determined through a combination of spectral fingerprinting and wave meter measurements. Values of ν_{obs} are listed in Table 1. The uncertainty in line position is indicated by the number in parentheses. In all cases, the transition frequencies were determined by collecting transient absorption signals at discrete IR wavelengths. Line positions for 4 transitions were determined by measuring Doppler-broadened line profiles (described in the next section). These line positions are reported with an uncertainty of $\delta\nu_{obs} = \pm 0.002$ cm^{-1}. Line positions for the remaining transitions were determined by scanning across the line profile in larger frequency steps than those used for the Doppler measurements and have a conservative uncertainty of $\delta\nu_{obs} = \pm 0.01$ cm^{-1}.

Table 1. Observed, calculated and predicted ν_3 R-branch N_2O line positions in (cm^{-1})

J	E_J [a]	ν_{obs}	ν_{calc} [b]	ν_{obs}-ν_{calc}	ν_{ext} (cm^{-1}) [c]	ν_{obs}-ν_{ext}
140	8202	2271.108(2)	2271.0908	0.017	2271.117	-0.009
160	10677	2266.197(2)	2266.1457	0.051	2266.199	-0.002
165	11344	2264.50(1)	2264.4482	0.05	2264.511	-0.01
167	11617	2263.79(1)	2263.7173	0.07	2263.785	0.01
169	11892	2263.02(1)	2262.9569	0.06	2263.030	-0.01
170	12031	2262.64(1)	2262.5655	0.07	2262.641	-0.001
180	13464	2258.348(2)	2258.2443	0.104	2255.350	-0.002
190	14973	2253.32(1)	2253.1800	0.14	2253.327	-0.007
195	15756	2250.544(2)	2250.3687	0.175	2250.540	0.004
203	17049	2245.71(1)	2245.4827	0.23	2245.703	0.007
205	17380	2244.43(1)	2244.1865	0.24	2244.420	0.010

a. Energies of N_2O (00^00) states based on effective Hamiltonian calculations from Ref [8].
b. Calculated transitions from Ref [8].
c. Transition frequencies based on extrapolation of a third order polynomial expansion from Ref [11].

The observed line positions are compared with the predicted frequencies ν_{calc} and ν_{ext} in Table 1 and Fig. 5. In all cases, the predicted frequencies are remarkably close to the observed values, given the large values of J and rotational energy. The extrapolated frequencies essentially match the observed values while the calculated frequencies show slight deviations with a small J-dependent increase.

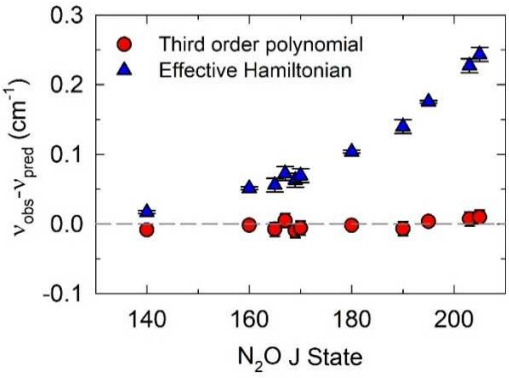

Fig. 5. Deviations of observed and predicted frequencies for N_2O high-J R-branch transitions.

The predicted frequencies from the extrapolated data are based on a perturbative treatment of rotational energy with the rigid rotor model as the reference system. This model does not explicitly include all vibrational modes of the molecule. The deviations for the extrapolated frequencies are surprisingly small, given the simplicity of the model.

The effective Hamiltonian accounts for rotation, vibration and their couplings and is therefore a much more realistic model than the perturbative expansion [8]. This model also successfully predicts the observed transitions. The small deviations from the observed transition frequencies correspond to less than one part in 10^4. At first glance, it is surprising that transitions from the effective Hamiltonian deviate from the observed transitions more than those for the simple perturbative expansion. It should be kept in mind, however, that data for high-J transitions were not available when the effective Hamiltonian calculations were performed. Our interpretation is that the effective Hamiltonian calculations are remarkably close to the observed frequencies, given the lack of experimental data for the high-J states at the time of the calculations. Being able to observe previously unknown rotational transitions with optical

centrifuge excitation will allow for further refinement of sophisticated effective Hamiltonian modeling.

3.2 Transient populations and line profiles of high-J N_2O (00^00)

The pulsed optical centrifuge excitation imparts large amounts of rotational energy to the sample and gives rise to time-dependent line intensities and profiles. Based on the bandwidth and intensity of the centrifuge pulse, we estimate that approximately 5% of the N_2O sample is prepared in states as high as $J = 310$, with rotational energy E_{rot} > 45000 cm^{-1}. The time evolution of the spectral lines gives information about the energy relaxation process. Here we report the time evolution of J-dependent number densities and Doppler-broadened line profiles for $J = 140$-195.

Fig. 6 shows N_2O (00^00) populations at two times following the optical centrifuge pulse. Transient absorption signals were converted to number densities by integrating over the Doppler profiles and using an IR path length of ℓ = 0.12 cm. At $t = 60$ ns, the population inversion created by the centrifuge pulse is clear with the J =195 population nearly 8-fold larger than that for $J =$ 92. At $t = 120$ ns, collisional energy transfer has doubled the population in $J = 92$ and reduced the $J = 195$ population by a factor of four.

State-specific number densities $N(J)$ were determined from transient absorption signals using $N(J) = -\ln(I_t/I_0)/(S_{296}(J)\, f(0)\, \ell) \cdot f_v f_J \cdot (\Delta\nu_{obs}/\Delta\nu_{296})$. Here, the transient absorption signals were converted to fractional transmitted intensities I_t/I_0, $S_{296}(J)$ is the line strength, $f(0)$ is the line shape parameter, ℓ is probe length in the interaction region, $f_v f_J$ is the fraction of molecules in the (00^00, J) state at 296 K, $\Delta\nu_{obs}$ is the transient line width at full-width half-maximum (FWHM) and $\Delta\nu_{296}$ is the FWHM line width at 296 K. Values of $S_{296}(J)/f_v f_J$

for the high-J transitions were determined from known line strength values and transition dipole moments using the approach of Gamache and Rothman. [17,18] The line strength values have a fractional uncertainty less than 0.01. The fractional uncertainties in I_t/I_0 and $\Delta\nu_{obs}$ are each less than 0.10; the overall fractional uncertainty in $N(J)$ values is less than 0.21. The number densities reported here are lower limits, since the IR path length could be a small as ℓ = 0.09 cm

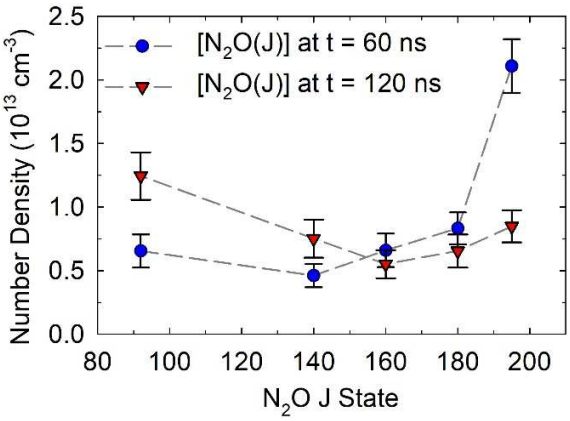

Fig. 6. J-dependent number densities for N_2O (00^00) at t = 60 and 120 ns after the optical centrifuge pulse.

based on the focusing characteristics of the centrifuge beam. Upper limit values are a factor of 1.3 larger than the reported values.

The line profiles for the R92-R195 transitions are Doppler-broadened and give information about J-specific translational energy distributions. Doppler profiles at t = 60 ns are shown in Fig. 7, along with Gaussian fitting results and residuals. From R92 to R195, the line widths become narrower, showing that the average translational energy decreases with increasing J-state. The peak intensities increase with J because of the population inversion.

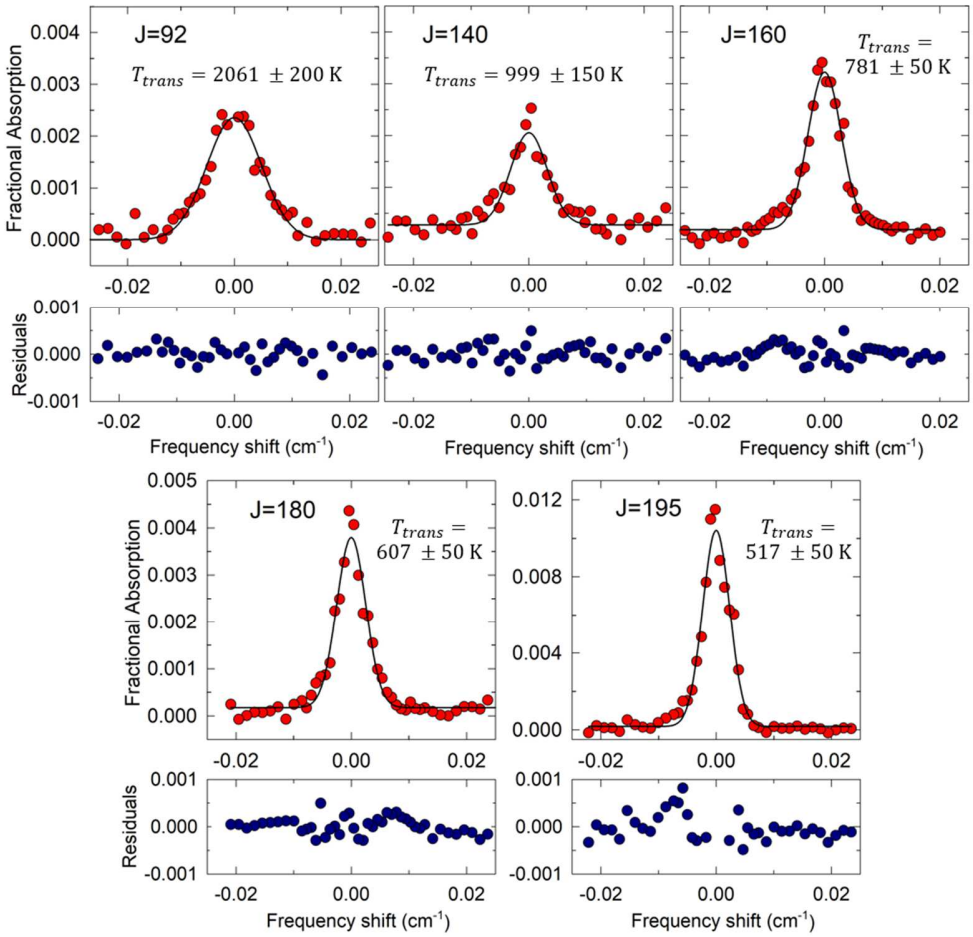

Fig. 7. Transient Doppler-broadened line profiles for selected N_2O states with $J = 92$-195. The data were collected at $t = 60$ ns after the centrifuge pulse. The higher-J states have larger signals and are shown with extended ranges of the y-axes.

The translational temperatures are plotted in Fig. 8 as a function of J-state for line profiles measured at t = 60 and 120 ns after the optical centrifuge pulse. For the states measured here, the translational temperatures are all greater than 300 K because of rotation-to-translational energy transfer. The J-dependence shows that higher J-states gain less translational energy than the lower J-states. The time-dependence shows that the translational energy gain continues to increase as more collisions occur. For the highest energy states, the population is gone before the line profiles narrow, showing that rotational relaxation is faster than translational quenching.

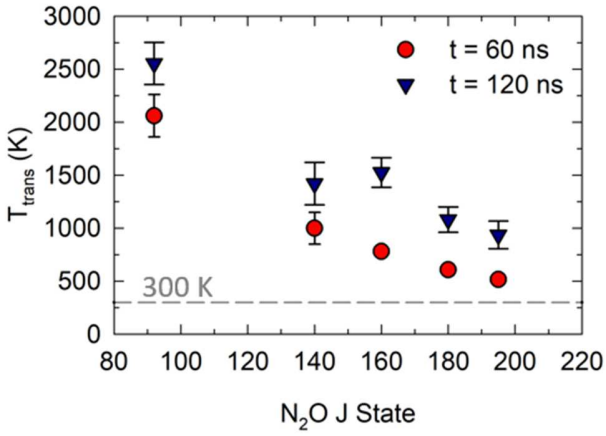

Fig. 8. Translational temperatures of N_2O at t = 60 and 120 ns after the centrifuge excitation.

The observed J-dependent data in Fig. 8 present a clear picture as to how collisions disperse the rotational energy of centrifuged molecules. Generally speaking, the relaxation of centrifuged molecules occurs by two limiting cases: resonant- and non-resonant energy transfer, depending on the J-state of their collision partner. The amount of translational energy in the collision products increases based on the rotational energy difference of the colliding molecules. In one case, near-resonant energy transfer occurs in collisions of two centrifuged molecules that

involve $\Delta J = \pm 1$ transitions. In this case, ΔE_{up} and ΔE_{down}values are nearly equal in magnitude, leaving negligible energy available for translation. On the other hand, collisions of centrifuged molecules with low-J molecules that have $\Delta J = \pm 1$ transitions result in large amounts of translational energy because the rotational energy transfer is non-resonant. Since rotational energy scales roughly as J^2, lower J-states gain more translational energy than states that are closer to the initial states prepared in the centrifuge. This behavior is clearly seen in Fig. 8. Of course, J-changing collisions are not limited to $\Delta J = \pm 1$ and collision products will have low translational energies as long as the rotational energy transfer is resonant or near resonant. Furthermore, the observation of translational broadening even for R195 at $t = 60$ ns indicates that the optical centrifuge initially prepares N_2O molecules well above $J = 200$. It should be possible in future studies to observe N_2O transitions with $J > 200$ by extending the IR tuning range in our transient spectrometer.

4. Conclusion

The work reported here demonstrates that the optical centrifuge is a powerful technique for populating high rotational states without having to perform experiments under high temperature conditions. When coupled with high-resolution transient IR absorption probing, new transition frequencies for high-J states can be measured with high accuracy. Here we report new R-branch transitions for N_2O (00^01-00^00) absorption up to R205. These measurements greatly extend previous observations of transitions up to R100 [1,6]. These results provide a direct comparison with advanced theoretical models of high temperature transitions, thereby helping to validate and refine the models. In a broader sense, the information gained from this study will enhance tools for characterizing remote and high temperature environments and for modeling of molecules in extreme rotational states.

Acknowledgments

The authors gratefully acknowledge Dr. Valerii I. Perevalov for providing calculated transition frequencies and Dr. Iouli E. Gordon for connecting us to the HighRus community. This work was generously supported by the National Science Foundation [NSF CHE-1800531]. HMO gratefully acknowledges an Ann Wiley Dissertation Fellowship from the Graduate School at the University of Maryland, College Park.

References

[1] Toth RA. N_2O vibration–rotation parameters derived from measurements in the 900–1090 and 1580–2380 cm^{-1} regions. J Opt Soc Am B 1987; 4:357.

[2] Esplin MP, Barowy WM, Huppi RJ, Vanasse GA. High resolution fourier spectroscopy of nitrous oxide at elevated temperatures. Mikrochim Acta 1988; 95:403–7.

[3] Morino I, Yamada KMT, Maki AG. Terahertz Measurements of Rotational Transitions in Vibrationally Excited States of N_2O. J Mol Spectrosc 1999; 196:131–8.

[4] Bailly D, Vervloet M. $^{14}N_2{}^{16}O$ in emission in the 4.5-μm Region: Transitions $\nu_1\nu^l_2\nu_3 \rightarrow \nu_1\nu^l_2(\nu_3 - 1)$ occurring between highly excited vibrational states. J Mol Spectrosc 2001; 209:207–15.

[5] Bailly D, Pirali O, Vervloet M. $^{14}N_2{}^{16}O$ emission in the 4.5 μM region: High excitation of the bending mode transitions $\nu_1\nu^l_2\nu_3 \rightarrow \nu_1\nu^l_2(\nu_3 - 1)$ with $(2\nu_1 + \nu_2) = 5$. J Mol Spectrosc 2003; 222:180–90.

[6] Yuan L, Toro C, Bell M, Mullin AS. Spectroscopy of molecules in very high rotational states using an optical centrifuge. Faraday Discuss 2011; 150:101–11.

[7] Ting W-J, Chang C-H, Chen S-E, Chen H-C, Shy J-T, Drouin BJ, et al. Precision frequency measurement of N_2O transitions near 4.5 μm and above 150 μm. J Opt Soc Am B 2014; 31:1954.

[8] Perevalov VI, Tashkun SA, Kochanov R V., Liu AW, Campargue A. Global modeling of the $^{14}N_2{}^{16}O$ line positions within the framework of the polyad model of effective Hamiltonian. J Quant Spectrosc Radiat Transf 2012; 113:1004–12.

[9] Tashkun SA, Perevalov VI, Lavrentieva NN. NOSD-1000, the high-temperature nitrous oxide spectroscopic databank. J Quant Spectrosc Radiat Transf 2016; 177:43–8.

[10] Hargreaves RJ, Gordon IE, Rothman LS, Tashkun SA, Perevalov VI, Lukashevskaya AA, et al. Spectroscopic line parameters of NO, NO_2, and N_2O for the HITEMP database. J Quant Spectrosc Radiat Transf 2019; 232:35–53.

[11] Gordon IE, Rothman LS, Hill C, Kochanov R V., Tan Y, Bernath PF, et al. The HITRAN2016 molecular spectroscopic database. J Quant Spectrosc Radiat Transf 2017; 203:3–69.

[12] Murray MJ, Ogden HM, Mullin AS. Importance of rotational adiabaticity in collisions of CO_2 super rotors with Ar and He. J Chem Phys 2018; 148:084310.

[13] Wright J, Corkum P, Ivanov M. Optical centrifuge for molecules. Phys Rev Lett 1999; 82:3420–3.

[14] Villeneuve DM, Aseyev SA, Dietrich P, Spanner M, Ivanov MY, Corkum PB. Forced molecular rotation in an optical centrifuge. Phys Rev Lett 2000; 85:542–5.

[15] Roncin J-Y. Intermolecular potential parameters of some electronic excited states of atoms and molecules. Chem Phys Lett 1969; 3:408-410.

[16] Yuan L, Teitelbaum SW, Robinson A, Mullin AS. Dynamics of molecules in extreme

rotational states. Proc Natl Acad Sci U S A 2011; 108:6872–7.

[17] Gamache RR, Rothman LS. Extension of the HITRAN database to non-LTE applications. JQRST 1992; 25: 505-525.

[18] Rothman LS, Rinsland CP, Goldman A, et al. The HITRAN molecular spectroscopic database and HAWKS (HITRAN atmospheric workstation): 1996 edition. J Quant Spectrosc Radiat Transf 1998; 60:665-710, Appendix A.